

# Hyperchaotic behavior of oscillator with cross-coupled transistor pair

Miroslav Rujzl, Jiri Petrzela  
Department of Radio Electronics  
Brno University of Technology  
Brno, Czech Republic  
xrujzl00@vutbr.cz, petrzelj@vutbr.cz

**Abstract**—This paper demonstrates existence of chaotic and hyperchaotic self-oscillations observed inside principal circuit topology of harmonic oscillator with cross-coupled transistor pair. Analyzed autonomous dynamical system is based on the simplified model of both transistors having nonlinear forward transconductance and divided resonant tanks. Numerical analysis covers calculation of two largest Lyapunov exponents, and long-time structural stability of generated strange attractors is verified via experimental construction and measurement of flow-equivalent simple lumped circuit.

**Index Terms**—chaos, chaotic oscillator, hyperchaos, Kaplan-Yorke dimension, Lyapunov exponent, strange attractor

## I. INTRODUCTION

Deterministic chaos can be roughly considered as a long-time unpredictable solution of differential equations having at least one scalar nonlinearity and without stochastic process. Since investigated mathematical model can be dimensionless chaos belongs to universal phenomena reported from nature sciences as well as technical disciplines.

Hyperchaotic self-oscillations belongs to a very complex dynamical phenomena associated with autonomous lumped electronic systems with at least four degrees of freedom [1]. Required dimensionality can be achieved willingly by circuit realization of prescribed mathematical model or via parasitic properties of used active devices. Experimental observations in the latter case can be misinterpreted as a thermal noise or similar stochastic process.

Analog design engineers are interested in construction of the chaotic oscillators for many decades. Special attention is usually devoted to the simplicity of final circuit, requirement of cheap and off-the-shelf active components, simple change of internal parameter of original math model, good agreement between theory and real measurement, structural stability of generated attractor, and reproducibility of practical results. Chaos-oriented enthusiasts are recently focused on fractional-order chaotic systems [2], chaotic oscillators with memristors and/or other mem-elements [3], hidden attractors revealed in mechanic or electrical engineering system [4], multi-stability [5], boundary surfaces [6], [7] and similar interesting topics.

This brief paper presents hyperchaotic oscillator that can be, from the circuit point of view, undoubtedly considered as one of the simplest examples. Since hyperchaotic behavior requires four degrees of freedom final network contains only

four accumulation elements. Also, the hyperchaotic motion is characterized by two positive Lyapunov exponents (LE), i.e., two neighboring trajectories simultaneously expands in two directions.

## II. MATHEMATICAL MODEL OF OSCILLATOR

Fundamental circuit structure of a harmonic oscillator with cross-coupled transistors is shown in Fig. 1a. In further text, this configuration will be analyzed as: firstly isolated, that is without external driving forces and load, and secondly, using transistors modelled exclusively by nonlinear forward transconductance approximated by a cubic polynomial. Doing so, the following set of ordinary differential equations can be derived for mentioned

$$\begin{aligned} C_1 \frac{dv_1}{dt} &= -i_{L1} - \hat{a}v_1^3 - \hat{b}v_2, & L_1 \frac{di_{L1}}{dt} &= v_1, \\ C_2 \frac{dv_2}{dt} &= -i_{L2} - \tilde{a}v_2^3 - \tilde{b}v_1, & L_2 \frac{di_{L2}}{dt} &= v_2 \end{aligned} \quad (1)$$

where state vector is  $\mathbf{x} = (v_1, i_{L1}, v_2, i_{L2})^T$ . Equilibrium points are all real solutions of nonlinear problem  $dx/dt = 0$ . Obviously, resulting algebraic equations have only a single zero solution, namely point  $\mathbf{x}_{eq} = (0, 0, 0, 0)^T$ . Since we are interested in the so-called self-excited strange attractors, origin needs to be the unstable fixed point. For further analysis, assume equivalency  $\hat{b} = \tilde{b} = b$ , i.e., forward transconductance of both transistors has the same slopes near zero. Jacobi matrix is a function of parameter  $b$ , and the local vector field geometry near origin is defined by the eigenvalues

$$\lambda_{1,2} = -\frac{1}{2}(b \pm \sqrt{b^2 - 4}), \lambda_{3,4} = \frac{1}{2}(b \pm \sqrt{b^2 - 4}) \quad (2)$$

Obviously, geometry near origin changes its nature for  $b = 2$  where eigenvalues are  $\lambda_{1,2} = -1, \lambda_{3,4} = 1$ . The lower values  $0 \leq b \leq 2$  lead to a geometrical combination of stable and unstable spiral (two eigen planes). As  $b$  decreases real parts of complex conjugated eigenvalues decrease as well. Limit case  $b = 0$  leads to a pair of the pure imaginary eigenvalues, that is  $\lambda_{1,2} = \pm j, \lambda_{3,4} = \pm j$ . The larger values of  $b$  results into flow movement along four eigen vectors (two stable and pair of unstable). Finally, negative values of parameter  $b$  do not give good physical sense since collector current of both transistors is reversed.

Models of both transistors are considered on the high level of abstraction, without the parasitic resistive and accumulation elements that include additional degrees of freedom and terms inside differential equations. This kind of modelling allows us to create a maximally general mathematical description of the autonomous dynamical system that covers large variety of real electronic circuits. In fact, “discovered” circuit represents two loss-less parallel resonant tanks with double-sided nonlinear coupling, see Fig. 1b. Nonzero cubic terms  $\hat{a}$ ,  $\tilde{a}$  are needed to obtain one- or two-dimensional volume expansion in the state space, that is, to observe chaotic and hyperchaotic steady state. To reach topologically simpler chaotic motion, one coupling transconductance can be linear.

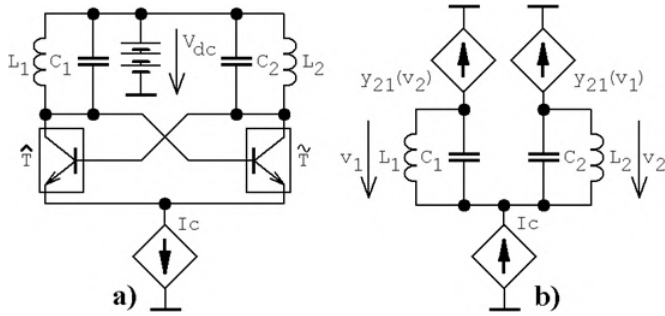


Fig. 1. Harmonic oscillator having cross-coupled pair of general transistors: a) fundamental network, b) simplified circuit with polynomial forward transconductance (two voltage controlled current sources)

### III. NUMERICAL ANALYSIS

Without losing a chance to observe complex random-like behavior, the normalized numerical values of all accumulation elements can be fixed unity, i.e.  $L_1 = L_2 = 1$  H and  $C_1 = C_2 = 1$  F, which corresponds to the fundamental oscillation frequency  $f = 159$  mHz. This is great advantage since oscillator theoretically generates chaotic or hyperchaotic waveforms for arbitrarily chosen time and impedance scaling. Therefore, there is no need to accept extreme differences between numerical values of capacitors and/or inductors.

In general, searching for the robust chaotic solution inside arbitrary dimensional hyperspace of system parameters can be understood as optimization task [8] utilizing flow quantifier as objective function. Shaping factors associated with nonlinear functions  $\hat{a}$ ,  $\hat{b}$ ,  $\tilde{a}$ ,  $\tilde{b}$  can be encoded into bit representation such that nature-inspired optimization routine can be used. Doing so, in our case, scanned hyperspace has only three dimensions with the additional volume restrictions  $\hat{a} < 0$  and  $\tilde{a} < 0$ .

Full grid searching approach provides several prosperous sets, for example  $\tilde{a} = -1$ ,  $\hat{b} = \tilde{b} = 1$ ,  $\hat{a} = -0.1$ . Numerical integration of dynamical system (1) by using a fourth order Runge-Kutta method, final time 1000 s and time step 10 ms having this set of internal parameters is provided in rainbow scaled colored images by means of fig. 2. Solution of both autonomous and driven dynamical system can be quantified and classified by using concept of LE. Number of LE corresponds to order of mathematical model. For

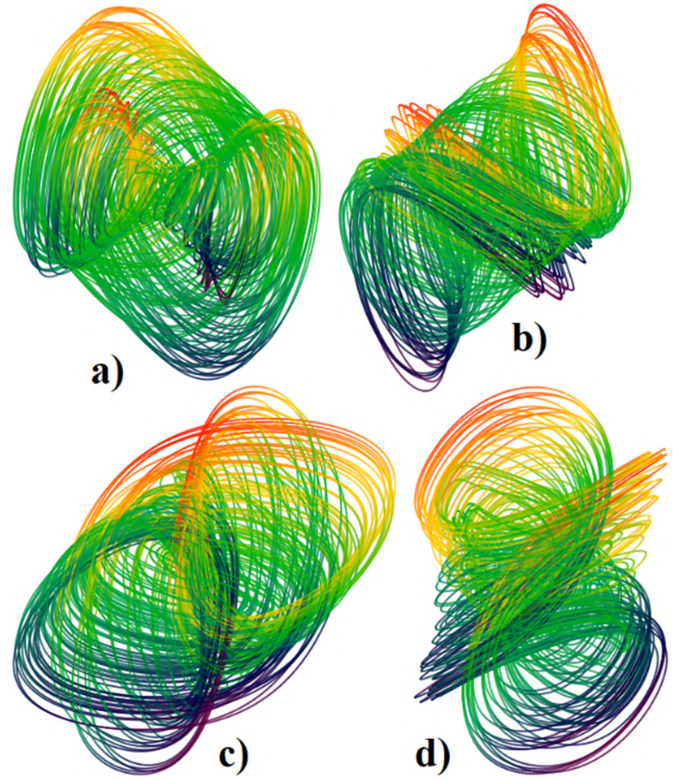


Fig. 2. Numerical integration of fourth order mathematical model (1), state space visualized from different 3D perspectives, a)  $v_1-i_{L1}-v_2$ , b)  $v_1-i_{L1}-i_{L2}$ , c)  $v_1-v_2-i_{L2}$ , d)  $i_{L1}-v_2-i_{L2}$ .

chaos, the largest LE needs to be positive, set of LE that results into the hyperchaotic movement possess two positive values. For dissipative dynamics, sum of all LE is negative. Topographically scaled surface-contour plot of the largest LE as two-dimensional function of  $\hat{a}$  and  $\tilde{a}$  for different values of parameter  $\hat{b} = \tilde{b} = b$  is provided via fig. 3. Black dots represent parameter places with distinguished hyperchaotic motion. The “most chaotic” case is obtained for the internal parameters  $\hat{a} = -0.23$ ,  $\tilde{a} = -0.03$ ,  $b = 4$  and has the largest LE about 0.184. The “most hyperchaotic” case can be observed for values  $\hat{a} = -0.01$ ,  $\tilde{a} = -0.65$ ,  $b = 4$  and is characterized by two positive LE, namely 0.138, 0.064. Of course, these quantities can be considered as local maxima since associated with a finite volume of parameter hyperspace addressed by calculation routine.

Figure 4 demonstrates the fundamental property of chaotic system, sensitivity of system solution to small uncertainties of group of initial conditions. To do this,  $10^4$  initial states (black dots) are generated with normal distribution and standard deviation  $10^{-2}$  around origin of a state space. After 1 s short time (red dots), 5 s medium time (green dots) and 50 s long time (blue dots) evolution the final states are stored and visualized. Obviously, long time end points associated with huge number of initial states will eventually fill entire strange attractor, which is only portion of 4D state space, leading to non-integer geometric dimension of evolved strange attractor.

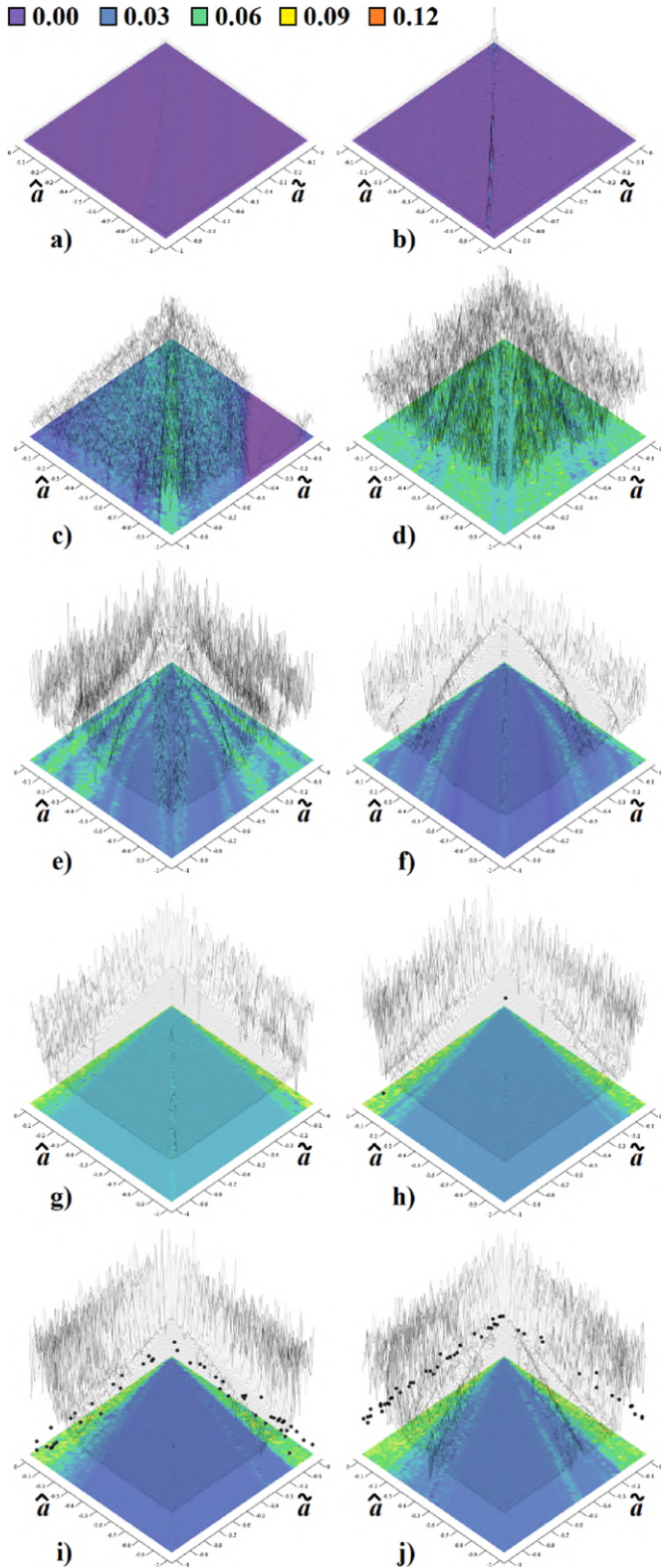


Fig. 3. Flow quantification via the largest LE, a)  $b = 0.1$ , b)  $b = 0.3$ , c)  $b = 0.5$ , d)  $b = 0.7$ , e)  $b = 1$ , f)  $b = 1.5$ , g)  $b = 2$ , h)  $b = 2.5$ , i)  $b = 3$ , j)  $b = 4$ .

System parameters are the same as adopted to numerically simulate fig. 2 (upper two plots provided) and for the “most hyperchaotic” set of the system parameters mentioned above (lower two plots).

Note that analyzed dynamical system is invariant under complete inversion of the system coordinates. In addition, geometry of the vector field suggests that there are several coexisting attractors, see fig. 5 for four examples. Orange trajectory evolves for initial conditions  $\mathbf{x}_0 = (0.1, 0, 0, 0)^T$ , blue orbit occurs if  $\mathbf{x}_0 = (1, 1, 0, 0)^T$ , green orbit can be observed thanks to the symmetry for  $\mathbf{x}_0 = (-1, -1, 0, 0)^T$ , and red attractor rises for  $\mathbf{x}_0 = (1, 0, 0, 0)^T$ . It has been verified numerically that dynamical system (1) exhibits multi-stability and covers both self-excited and the so-called hidden chaotic attractors [9].

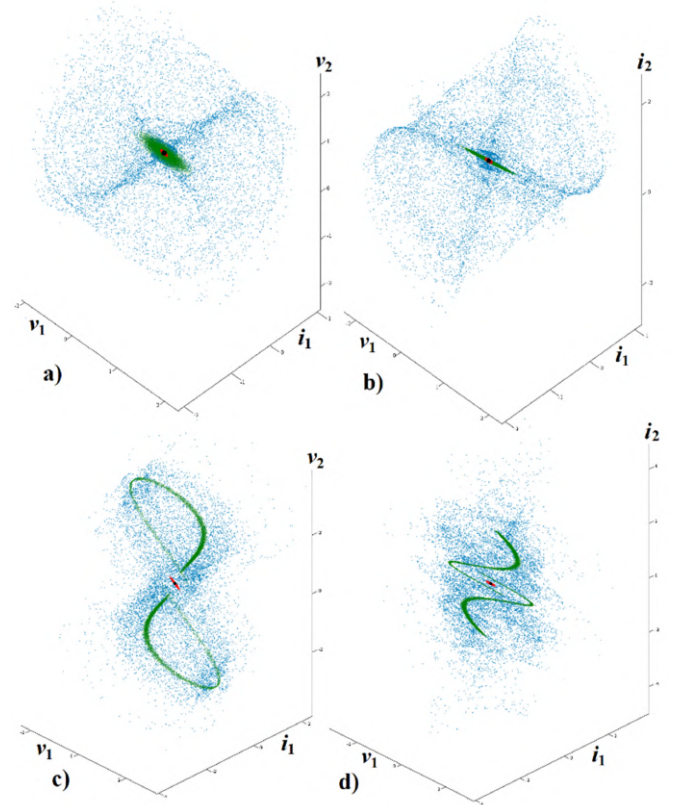


Fig. 4. Sensitivity of analyzed system solution to the small deviations in the initial conditions, plotted in state space cubes: a)  $v_1-i_{L1}-v_2$ , b)  $v_1-i_{L1}-i_{L2}$ , c)  $v_1-i_{L1}-v_2$ , d)  $v_1-i_{L1}-i_{L2}$ . For details, consult corresponding text passage.

#### IV. EXPERIMENTAL VERIFICATION

Synthesis of the fully analog chaotic oscillators based on known mathematical description is easily solvable problem having multiple correct solutions. Many papers were already devoted to this task, for example cookbooks [10], [11]. Probably the most straightforward design approach is based on analog computer concept where necessary mathematical operations are done by using three building blocks: inverting summing integrator, differential amplifier (inverting

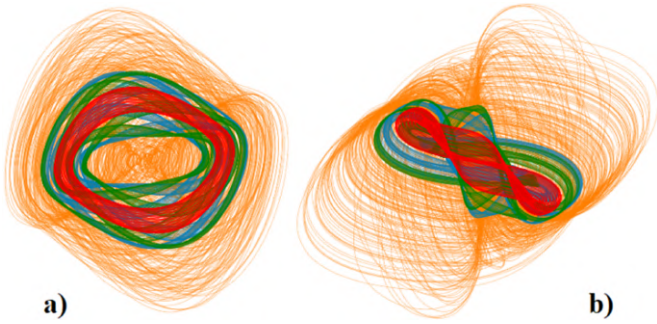


Fig. 5. Coexistence of several different state attractor within the state space, plane projection: a)  $v_1-i_{L1}-v_2$ , b)  $v_1-v_2-i_{L2}$ .

summing amplifier being its special case), and two-port with desired nonlinear transfer function. Time domain waveforms associated with the state attractors that are expected to be generated by designed circuit do not have significant DC frequency components. Thus, the active operational amplifier-based realization of the lossless inverting summing integrators can be adopted. Final schematic including numerical values of the passive elements is provided in fig. 6. For experimental measurement, time constant of integrators were chosen  $\tau = RC = 10^4 \cdot 10^{-8} = 100 \mu s$ . To implement the cubic polynomial transfer functions, four quadrant analog multipliers AD633 were utilized. Chaotic oscillator contains seven commercially available integrated circuits: single cheap TL084, pair of AD844 and four AD633. In given schematic, TZ represents node initially dedicated for compensation of frequency curves.

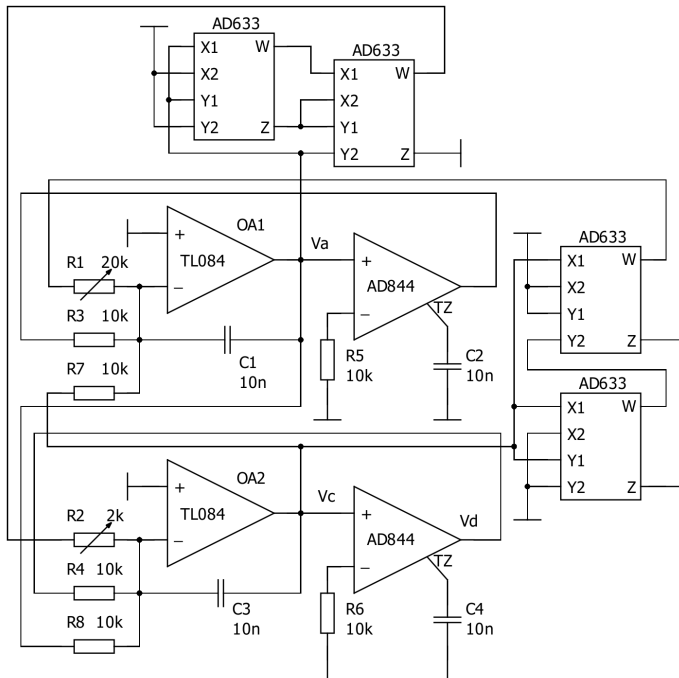
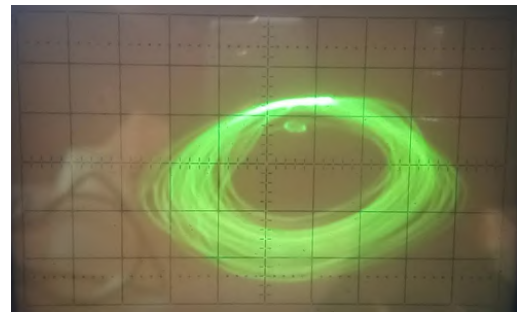
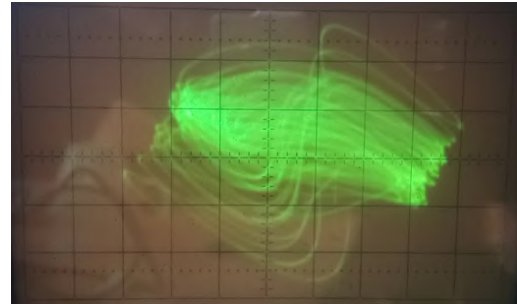


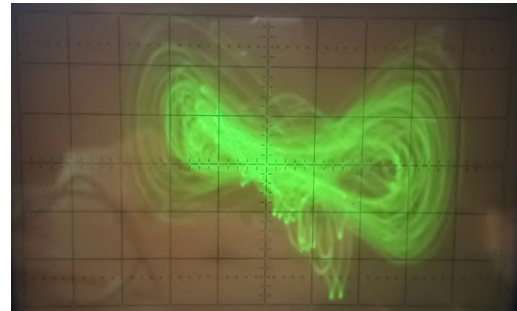
Fig. 6. Detailed circuitry implementation of analog chaotic oscillator based on harmonic oscillator with cross-coupled transistors.



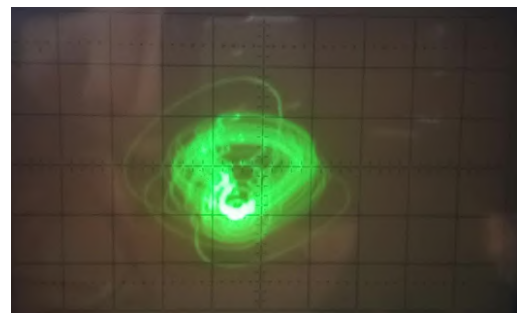
(a)



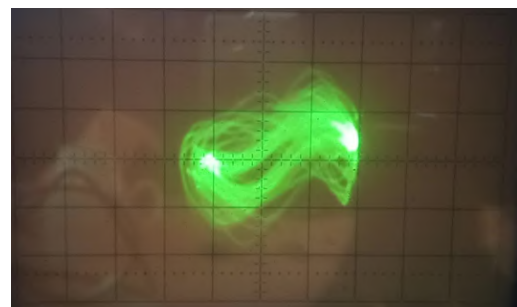
(b)



(c)



(d)



(e)

Fig. 7. Experimental verification of the chaotic oscillator, plane projection: a)  $v_a-v_b$ , b)  $v_a-v_d$ , c)  $v_a-v_c$ , d)  $v_c-v_d$ , e)  $v_b-v_c$

Behavior of designed electronic system is described by following set of ordinary differential equations

$$\begin{aligned} -C_1 \frac{dv_a}{dt} &= \frac{v_b}{R_3} + \frac{v_c}{R_7} - \frac{K^2}{R_1} v_c^3, & C_2 \frac{dv_b}{dt} &= \frac{v_a}{R_5}, \\ -C_3 \frac{dv_c}{dt} &= \frac{v_d}{R_8} + \frac{v_a}{R_4} - \frac{K^2}{R_2} v_a^3, & C_4 \frac{dv_d}{dt} &= \frac{v_c}{R_6} \end{aligned} \quad (3)$$

where  $K = 0.1$  is internally trimmed constant of multipliers.

Chaotic waveforms contain a huge number of harmonics and has continuous broad-band frequency spectrum. Selected oscilloscope screenshots are provided in fig. 7. Observed experimental results are in good accordance with theoretical assumptions. Different route-to-chaos scenarios can be traced via change of the system parameters  $\hat{a}$  or  $\tilde{a}$ , i.e. by adjusting variable resistors  $R_1$  or  $R_2$ .

## V. CONCLUSION

This paper briefly describes simple transformation process from harmonic oscillator based on the cross-coupled transistor pair into hyperchaotic oscillator. It has been numerically proved that change of output current orientation associated with transconductance of both transistors also leads to the complex behavior including interesting, strange attractors.

## ACKNOWLEDGMENT

This paper is realized within the project Quality Internal Grants of BUT (KInG BUT), Reg. No. CZ.02.2.69/0.0/0.0/19\_073/0016948, which is financed from the OP RDE.

## REFERENCES

- [1] J. Petrzela, and L. Polak, "Hyperchaotic self-oscillations of two-stage class C amplifier with generalized transistors," *IEEE Access*, vol. 9, pp. 62182–62194, 2021.
- [2] J. Yao, K. Wang, P. Huang, L. Chen, and J. A. Tenreiro-Machado, "Analysis and implementation of fractional-order chaotic system with standard components," *Journal of Advanced Research*, vol. 25, pp. 97–109, 2020.
- [3] K. Rajagopal, C. Li, F. Nazarimehr, A. Karthikeyan, P. Duraisamy, and S. Jafari, "Chaotic dynamics of modified Wien bridge oscillator with fractional order memristor," *Radioengineering*, vol. 28, pp. 165–174, 2019.
- [4] N. V. Kuznetsov, G. A. Leonov, M. V. Yuldashev, R. V. Yuldashev, "Hidden attractors in dynamical models of phase-locked loop circuits: limitations of simulation in MATLAB and SPICE," *Communications in Nonlinear Science and Numerical Simulation*, vol. 51, pp. 39–49, 2017.
- [5] V.-T. Pham, D. S. Ali, N. M. G. Al-Saidi, K. Rajagopal, F. E. Alsaadi, and S. Jafari, "A novel mega-stable chaotic circuit," *Radioengineering*, vol. 29, pp. 140–146, 2020.
- [6] M. Guzan, "Boundary surface of a ternary memory in the absence of limit cycles," In *Proceedings of 22nd International Conference Radioelektronika 2012*, April 17–18, Brno, Czech Republic, 2012.
- [7] M. Guzan, P. Kovac, I. Kovacova, M. Beres, A. Gladyr, "Boundary surface of Chua's circuit in 3D state space," In *Proceedings of International Conference on Modern Electrical and Energy Systems*, November 15–17, Kremenchuk, Ukraine, 2017.
- [8] A. Silva-Juarez, E. Tlelo-Cuautle, Gerardo de la Fraga, L., and R. Li, "Optimization of the Kaplan-Yorke dimension in fractional-order chaotic oscillators by metaheuristics," *Applied Mathematics and Computation*, vol. 394, pp. 125831, 2021.
- [9] S. Jafari, A. Ahmadi, A. J. M. Khalaf, H. Abdolmohammadi, V.-T. Pham, and F. Alsaadi, "A new hidden chaotic attractor with extreme multi-stability," *AEU-International Journal of Electronics and Communications*, vol. 89, pp. 131–135, 2018.

- [10] M. Itoh, "Synthesis of electronic circuits for simulating nonlinear dynamics," *International Journal of Bifurcation and Chaos*, vol. 11, pp. 605–653, 2001.
- [11] J. Petrzela, T. Gotthans, and M. Guzan, "Current-mode network structures dedicated for simulation of dynamical systems with plane continuum of equilibrium," *Journal of Circuits, Systems and Computers*, vol. 27, pp. 1830004, 2018.